

Isogeometric Analysis for Compressible Flow Problems in Industrial Applications

Matthias Möller

Delft Institute of Applied Mathematics, Numerical Analysis
Delft University of Technology

I³MS Seminar, 13 November 2017, CATS@RWTH Aachen

Numerical Analysis group: Prof.dr.ir. Kees Vuik, Kees Oosterlee

- 12 assistant/associated professors, 30 PhDs, 5 guest researchers
- Industrial flows, FSI, biomath, finance, iterative solvers, HPC, ...

My research team:

- J. Hinz: *IgA-based elliptic grid generation for industrial applications*
- R. Tielen: *IgA-inspired high-order material point method*
- J. v.d. Meer: *foam enhanced oil recovery*
- A. Jaeschke (TU Lodz, PL): *IgA in turbomachinery applications*

My own research interests:

- High-order high-resolution FEM/IgA schemes and efficient solvers for compressible flow problems, hardware-oriented numerics on unconventional hardware, quantum computing

Overview

① Introduction

Scientific computing from a hardware perspective
Isogeometric design-simulation-optimization loop

② Elliptic 'grid' generation

[J. Hinz]

Planar parameterizations
Volumetric parameterizations

③ Compressible flow solver

[A. Jaeschke]

Problem formulation
Linearized FCT limiter
Numerical examples

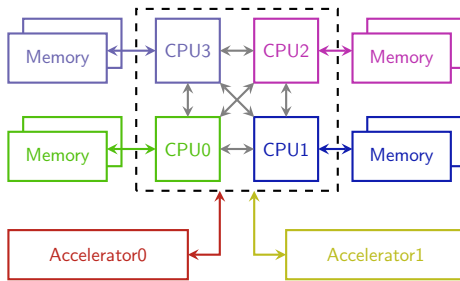
④ Implementation aspects

Meta-programming techniques for heterogeneous HPC

Scientific computing from a hardware perspective

Today: Heterogeneous compute hardware at system and node level

- Distributed cluster systems with heterogeneous compute nodes
 - Multi-core CPUs: Intel 28, AMD 32, ARM 48, IBM 16x12
 - Many-core accelerators: GPUs, Intel MICs, FPGAs, ...
 - Memory subsystem is the bottleneck in data-intensive applications



Scientific computing from a hardware perspective

Today: Heterogeneous compute hardware at system and node level

- Distributed cluster systems with heterogeneous compute nodes
 - Multi-core CPUs: Intel 28, AMD 32, ARM 48, IBM 16x12
 - Many-core accelerators: GPUs, Intel MICs, FPGAs, ...
 - Memory subsystem is the bottleneck in data-intensive applications

Future trends: 'novel' hardware architectures and paradigm shifts

- In-memory-computing for data-intensive applications (DBs, FEM?)
- Data-flow computing in space *vs.* control-flow computing in time
- Special-purpose accelerators: analogue or quantum computers

Scientific computing from a hardware perspective

Today: Heterogeneous compute hardware at system and node level

- Distributed cluster systems with heterogeneous compute nodes
 - Multi-core CPUs: Intel 28, AMD 32, ARM 48, IBM 16x12
 - Many-core accelerators: GPUs, Intel MICs, FPGAs, ...
 - Memory subsystem is the bottleneck in data-intensive applications

Future trends: 'novel' hardware architectures and paradigm shifts

- In-memory-computing for data-intensive applications (DBs, FEM?)
- Data-flow computing in space *vs.* control-flow computing in time
- Special-purpose accelerators: analogue or quantum computers

Philosophy: Bottom-up design of hardware-oriented numerics *for* next-gen hardware instead of squeezing existing methods *into* it.

An example of data-flow computing in space

Example: 2d Poisson equation

- IgA with tensor-product B-spline basis functions of order $p = 2$.
- Matrix-free iterative CG/BiCGStab solver

¹CMAME 316, (2017) 606-622.

An example of data-flow computing in space

Example: 2d Poisson equation

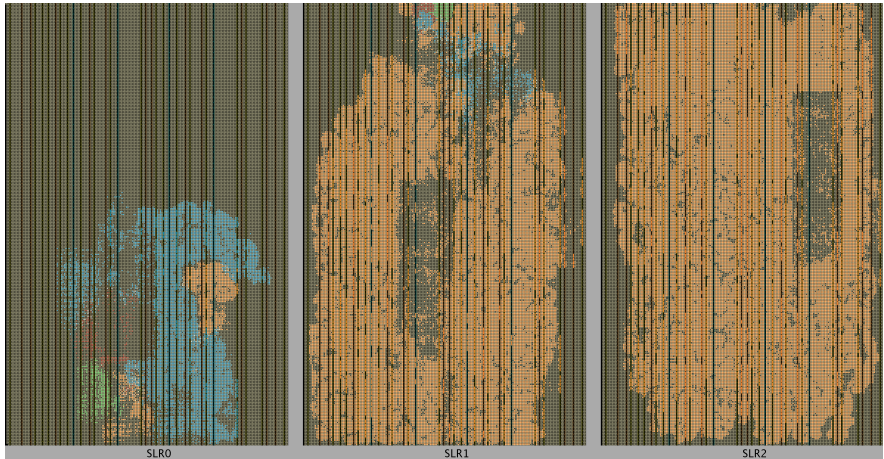
- IgA with tensor-product B-spline basis functions of order $p = 2$.
- Matrix-free iterative CG/BiCGStab solver
- Weighted quadrature approach by Calabrò et al.¹ is used for the on-the-fly generation matrix entries in the SpMv subroutine

$$S_{i,j} = \sum_{\alpha,\beta=1}^d \int_{[0,1]^2} g_{\alpha,\beta}(\xi) \partial_\beta \hat{B}_j(\xi) \left(\partial_\alpha \hat{B}_i(\xi) d\xi \right)$$

$$\approx \sum_{\alpha,\beta=1}^d \mathfrak{Q}_{\alpha,\beta,i}^{\text{WQ}} \left(g_{\alpha,\beta}(\cdot) \partial_\beta \hat{B}_j(\cdot) \right)$$

¹CMAME 316, (2017) 606-622.

An example of data-flow computing in space



Site Types

- SLICE
- URAM288
- DSP48E2
- RAMB18

Kernels

- paddingKernel [SLR1, SLR0]
- matrixKernel [SLR2, SLR1, SLR0]
- paddingKernel2 [SLR1, SLR0]
- vectorKernel [SLR1, SLR0]

■ Shared sites

R.v.Nieuwpoort: Implementation of the weighted quadrature approach by Tani et al. on MAX5 Lima DFE

An example of analogue computing

Example: 1d Poisson equation

- Solution to the linear system $Ax = b$ can be interpreted as the steady state limit of the initial value problem

$$\frac{dx(t)}{dt} = b - Ax(t), \quad x(0) = x_0$$

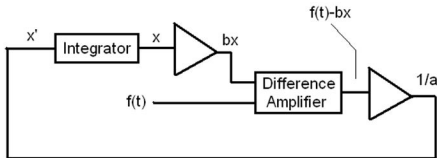
An example of analogue computing

Example: 1d Poisson equation

- Solution to the linear system $Ax = b$ can be interpreted as the steady state limit of the initial value problem

$$\frac{dx(t)}{dt} = b - Ax(t), \quad x(0) = x_0$$

- Analogue computers are efficient in modelling differential equations using op-amps but very expensive to operate at large scales



An example of analogue computing

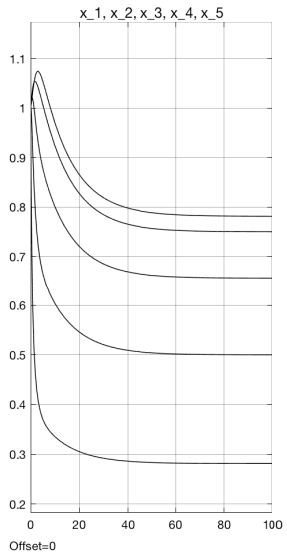
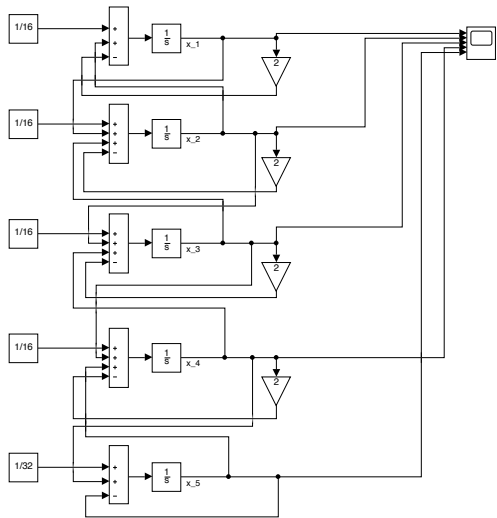
Example: 1d Poisson equation

- Solution to the linear system $Ax = b$ can be interpreted as the steady state limit of the initial value problem

$$\frac{dx(t)}{dt} = b - Ax(t), \quad x(0) = x_0$$

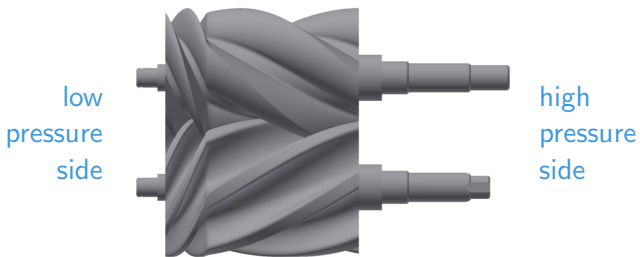
- Analogue computers are efficient in modelling differential equations using op-amps but very expensive to operate at large scales
- Analogue computing can bring to new ideas, e.g., for data-flow computing architectures like FPGAs and quantum computers

An example of virtual analogue computing



Vision: Isogeometric DSO loop

Our objective is to develop an IGA toolbox for the efficient **Design, Simulation and Optimization** of screw machines with variable pitches



Courtesy of Andreas Brümmer, Dortmund University of Technology.

Collaboration: TU Kaiserslautern, TU Dortmund, TU Delft, JKU Linz

Vision: Isogeometric DSO loop

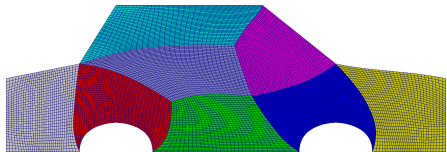
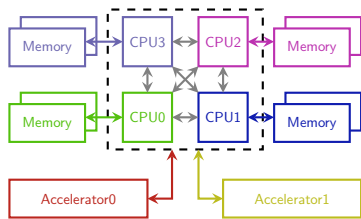
Challenges:

- Rotating geometries with tiny gaps ($< 0.4\text{mm}$) between rotors
- Multi-physics problem: compressible flows, thermal deformation, ...
- Prevent topology changes of the multi-patch structure

Design criteria:

- High-resolution capturing of shocks and discontinuities
- Support for current and future HPC platforms
- KISS (no unmaintainable hacks)

A 'novel' hardware-oriented numerics approach



Multi-patch domain parameterization for isogeometric analysis
in G+Smo by Buchegger and Jüttler CAD 82, p. 2-12, 2017

Multi-patch Isogeometric Analysis:

- B-spline based iso-parametric FEM on unstructured coarse grid
- Fully structured high-order discretizations with hardware-optimized implementations on individual patches
- Multi-patch DG-coupling with minimal communication overhead

Overview

① Introduction

Scientific computing from a hardware perspective
Isogeometric design-simulation-optimization loop

② Elliptic 'grid' generation

[J. Hinz]

Planar parameterizations
Volumetric parameterizations

③ Compressible flow solver

[A. Jaeschke]

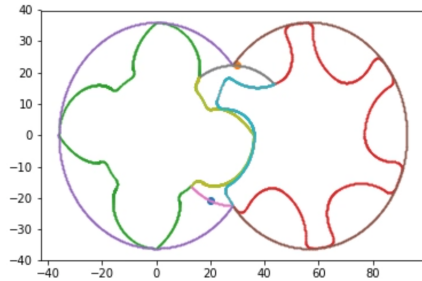
Problem formulation
Linearized FCT limiter
Numerical examples

④ Implementation aspects

Meta-programming techniques for heterogeneous HPC

Sliding grid technology - planar case

Approach: Create multi-patch parameterizations of fluid domain (O- or C-type + separator) and let the rotors slide along the inner boundaries



Pros: no topology changes, conforming/'nested' nonconforming patches
Cons: Change of separator parameterization is not continuous in time

Elliptic 'grid' generation

Algorithm²: Given a *point cloud* describing the patch boundary create an analysis-suitable *parameterization* $\hat{G}_f : [0, 1]^2 \rightarrow \Omega_f$ as follows:

²J. Hinz, MM, C. Vuik, submitted to GMP 2018

Elliptic 'grid' generation

Algorithm²: Given a *point cloud* describing the patch boundary create an analysis-suitable *parameterization* $\hat{G}_f : [0, 1]^2 \rightarrow \Omega_f$ as follows:

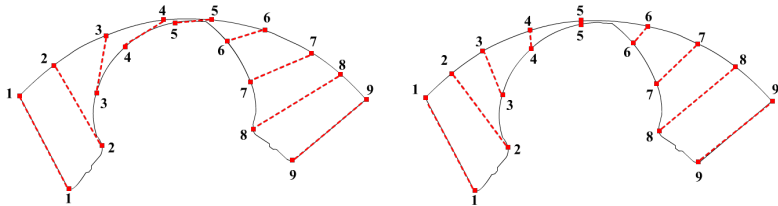
- ① Generate boundary parameterizations $\gamma_k, k \in \{N, S, E, W\}$

²J. Hinz, MM, C. Vuik, submitted to GMP 2018

Elliptic 'grid' generation

Algorithm²: Given a *point cloud* describing the patch boundary create an analysis-suitable *parameterization* $\hat{G}_f : [0, 1]^2 \rightarrow \Omega_f$ as follows:

- ① Generate boundary parameterizations $\gamma_k, k \in \{N, S, E, W\}$
- ② Reparameterize opposite boundaries at 'small-gap regions' by constrained cord-length parameterization algorithm



²J. Hinz, MM, C. Vuik, submitted to GMP 2018

Elliptic 'grid' generation

Algorithm²: Given a *point cloud* describing the patch boundary create an analysis-suitable *parameterization* $\hat{G}_f : [0, 1]^2 \rightarrow \Omega_f$ as follows:

- ① Generate boundary parameterizations $\gamma_k, k \in \{N, S, E, W\}$
- ② Reparameterize opposite boundaries at 'small-gap regions' by constrained cord-length parameterization algorithm
- ③ Compute union of basis functions of opposite boundaries

²J. Hinz, MM, C. Vuik, submitted to GMP 2018

Elliptic 'grid' generation

Algorithm²: Given a *point cloud* describing the patch boundary create an analysis-suitable *parameterization* $\hat{G}_f : [0, 1]^2 \rightarrow \Omega_f$ as follows:

- ① Generate boundary parameterizations $\gamma_k, k \in \{N, S, E, W\}$
- ② Reparameterize opposite boundaries at 'small-gap regions' by constrained cord-length parameterization algorithm
- ③ Compute union of basis functions of opposite boundaries
- ④ Generate a bi-variate parameterization by solving with IgA

$$\begin{aligned}\hat{g}_{22}x_{\xi\xi} - 2\hat{g}_{12}x_{\xi\eta} + \hat{g}_{11}x_{\eta\eta} &= 0 \\ \hat{g}_{22}y_{\xi\xi} - 2\hat{g}_{12}y_{\xi\eta} + \hat{g}_{11}y_{\eta\eta} &= 0\end{aligned}\quad s.t. \quad \hat{G}_{m,f} \Big|_{\hat{\Gamma}_{m,f}} = \Gamma_{m,f}$$

²J. Hinz, MM, C. Vuik, submitted to GMP 2018

Elliptic 'grid' generation

Algorithm²: Given a *point cloud* describing the patch boundary create an analysis-suitable *parameterization* $\hat{G}_f : [0, 1]^2 \rightarrow \Omega_f$ as follows:

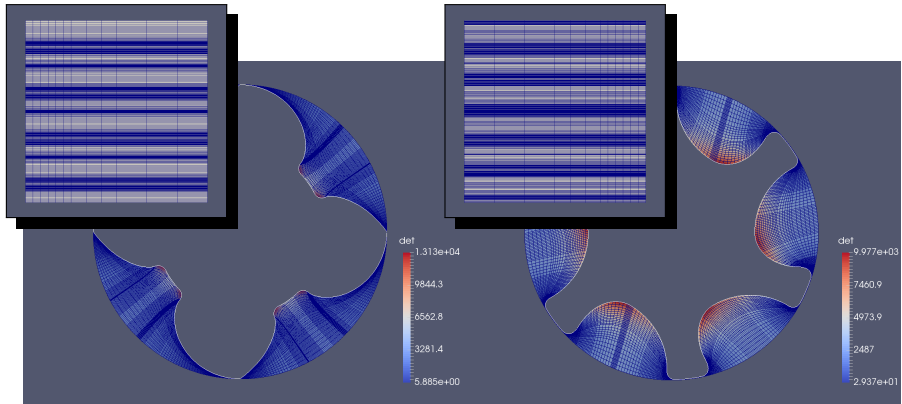
- ① Generate boundary parameterizations $\gamma_k, k \in \{N, S, E, W\}$
- ② Reparameterize opposite boundaries at 'small-gap regions' by constrained cord-length parameterization algorithm
- ③ Compute union of basis functions of opposite boundaries
- ④ Generate a bi-variate parameterization by solving with IgA

$$\begin{aligned}\hat{g}_{22}x_{\xi\xi} - 2\hat{g}_{12}x_{\xi\eta} + \hat{g}_{11}x_{\eta\eta} &= 0 \\ \hat{g}_{22}y_{\xi\xi} - 2\hat{g}_{12}y_{\xi\eta} + \hat{g}_{11}y_{\eta\eta} &= 0\end{aligned}\quad s.t. \quad \hat{G}_{m,f} \Big|_{\hat{\Gamma}_{m,f}} = \Gamma_{m,f}$$

- ⑤ Adaptively refine knot spans where $\det D\hat{G}_{m,f} \leq \text{tol}$ and repeat

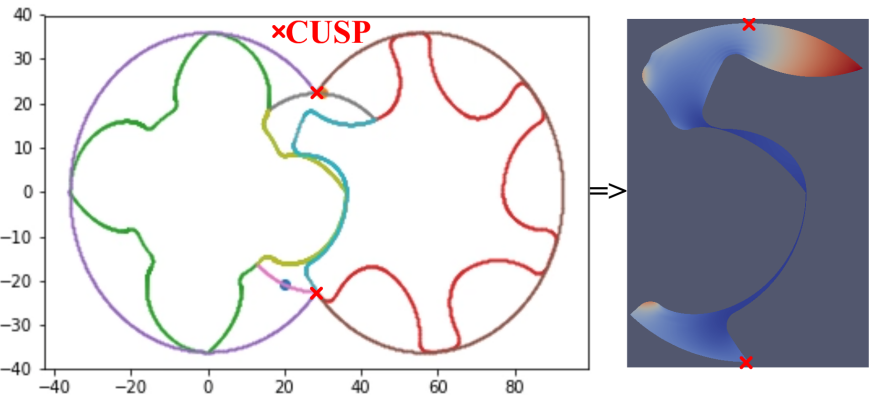
²J. Hinz, MM, C. Vuik, submitted to GMP 2018

Parameterizations of male/female rotors



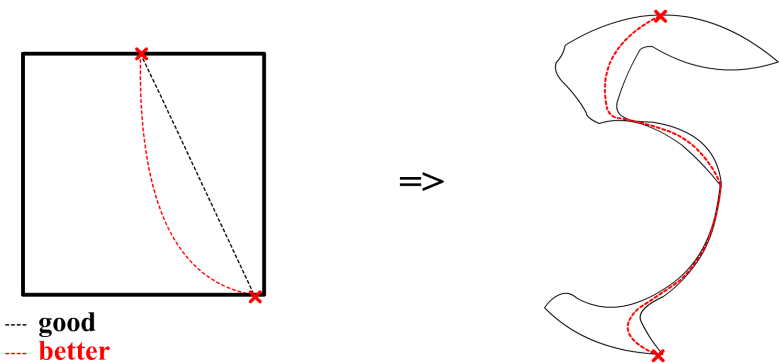
One-patch separator geometry

Approach: Create parameterization for separator geometry



One-patch separator geometry

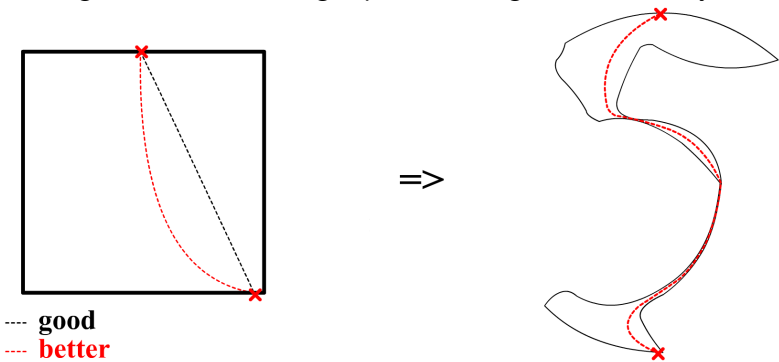
Approach: Create parameterization for separator geometry, compute splitting curve



--- good
--- better

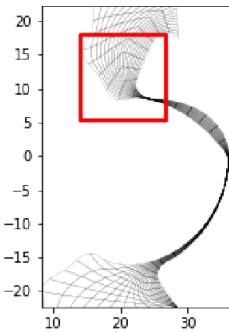
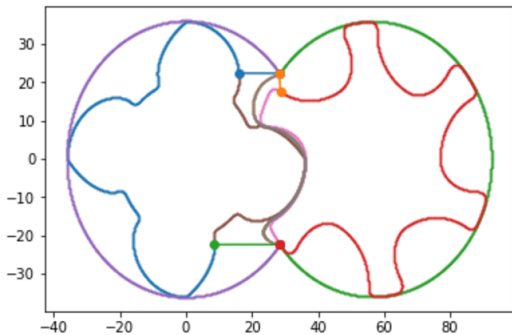
One-patch separator geometry

Approach: Create parameterization for separator geometry, compute splitting curve and (a) update point cloud and regenerate O-grids, or (b) adjust O-grids to match along separator using linear elasticity.



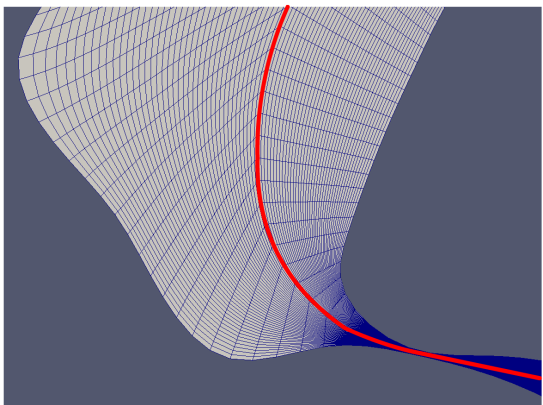
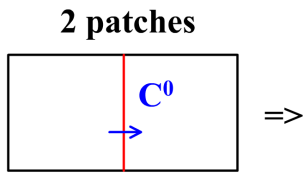
Two-patch separator geometry

Approach: Create two-patch separator



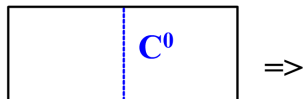
Two-patch separator geometry

Approach: Create two-patch separator with C^0 continuity along splitting curve

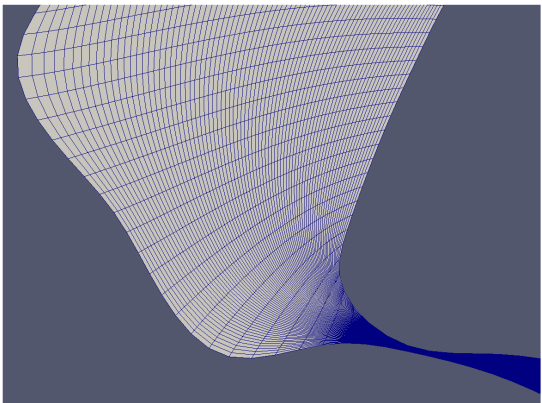


Two-patch separator geometry

Approach: Create two-patch separator with C^0 continuity along splitting curve, combine into one patch and run 'repair' algorithm.

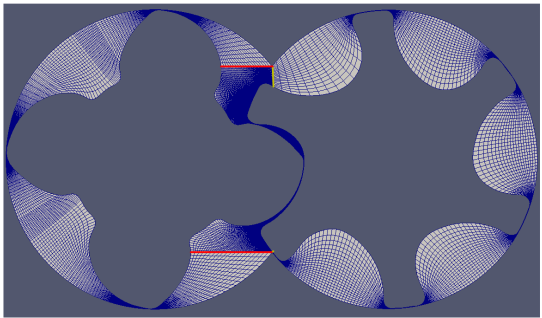
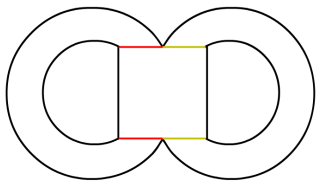


run algorithm that allows for C^0
but requires bijective initial guess



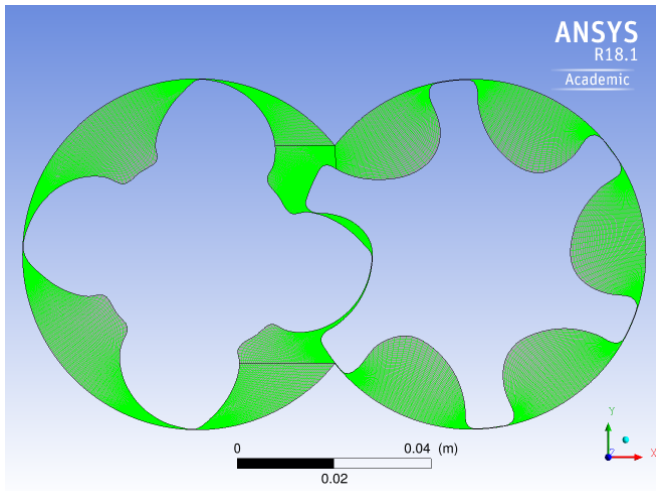
Two-patch separator geometry

Approach: Create two-patch separator with C^0 continuity along splitting curve, combine into one patch and run 'repair' algorithm.



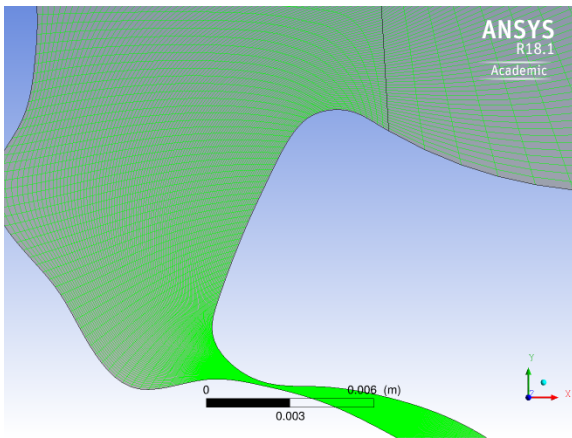
Generation of classical FEM meshes

Approach: Evaluate parameterization in parameter domain to obtain block-structured/unstructured (globally conforming) grids



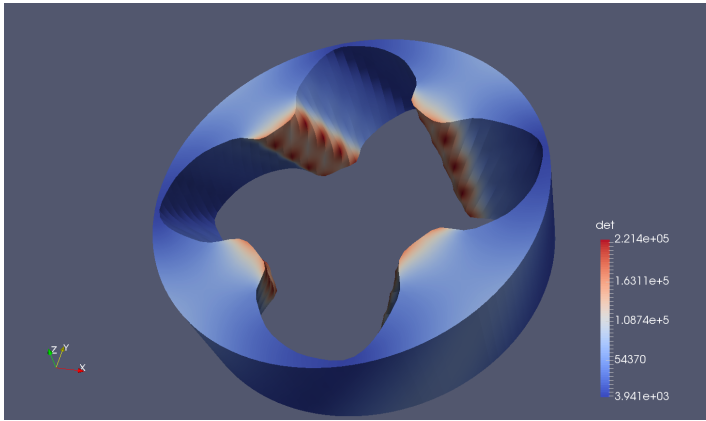
Generation of classical FEM meshes

Approach: Evaluate parameterization in parameter domain to obtain block-structured/unstructured (globally conforming) grids



Volumetric grid generation

Approach: Interpolate (linearly) between planar parameterizations at different rotation angles to generate static volumetric parameterization



Overview

① Introduction

Scientific computing from a hardware perspective
Isogeometric design-simulation-optimization loop

② Elliptic 'grid' generation

[J. Hinz]

Planar parameterizations
Volumetric parameterizations

③ Compressible flow solver

[A. Jaeschke]

Problem formulation
Linearized FCT limiter
Numerical examples

④ Implementation aspects

Meta-programming techniques for heterogeneous HPC

Compressible Euler equations

Divergence form

$$U_{,t} + \nabla \cdot \mathbf{F}(U) = 0$$

Quasi-linear form

$$U_{,t} + \mathbf{A}(U) \cdot \nabla U = 0$$

Conservative^a **variables**, inviscid **fluxes**, flux-Jacobian **matrices**

$$U = \begin{bmatrix} \rho \\ \rho\mathbf{v} \\ \rho E \end{bmatrix}, \quad \mathbf{F} = \begin{bmatrix} \rho\mathbf{v} \\ \rho\mathbf{v} \otimes \mathbf{v} + \mathcal{I}p \\ \mathbf{v}(\rho E + p) \end{bmatrix}, \quad \mathbf{A} = \frac{\partial \mathbf{F}}{\partial U}$$

Equation of state (here for an ideal gas)

$$p = (\gamma - 1) \left(\rho E - \frac{1}{2} \rho \|\mathbf{v}\|^2 \right), \quad \gamma = C_p / C_v$$

^aSimilar formulations exist for primitive and entropy variables

Divergence form

$$U_{,t} + \nabla \cdot \mathbf{F}(U) = 0$$

Quasi-linear form

$$U_{,t} + \mathbf{A}(U) \cdot \nabla U = 0$$

Conservative^a **variables**, inviscid **fluxes**, flux-Jacobian **matrices**

$$U = \begin{bmatrix} u_1 \\ \vdots \\ u_{d+2} \end{bmatrix}, \quad \mathbf{F} = \begin{bmatrix} f_1^1 & \dots & f_1^d \\ \vdots & \ddots & \vdots \\ f_{d+2}^1 & \dots & f_{d+2}^d \end{bmatrix}, \quad \mathbf{A} = \frac{\partial \mathbf{F}}{\partial U}$$

Notation

$$\mathbf{f}_k = [f_k^1, \dots, f_k^d], \quad \mathbf{f}^I = \begin{bmatrix} f_1^I \\ \vdots \\ f_{d+2}^I \end{bmatrix}$$

^aSimilar formulations exist for primitive and entropy variables

Galerkin ansatz

Find solution U at fixed time t s.t. for all W

$$\int_{\Omega} WU_{,t} - \nabla W \cdot \mathbf{F}(U) \, d\Omega + \int_{\Gamma} WF^b(U, \cdot) \, ds = 0$$

with boundary fluxes

$$F^b = \begin{cases} [0, pn_1, pn_2, pn_3, 0]^\top & \text{at solid walls} \\ \frac{1}{2}(F_n(U_-) + F_n(U_+)) - \frac{1}{2}|A_n(\text{Roe}(U_-, U_+))| & \text{otherwise} \end{cases}$$

Fletcher's group formulation³

$$U_h = \sum_j B_j(\mathbf{x})U_j(t), \quad \mathbf{F}_h = \sum_j B_j(\mathbf{x})\mathbf{F}_j(t), \quad \mathbf{F}_j = \mathbf{F}(U_j)$$

³Fletcher, CMAME 37 (1983) 225–244.

SpMV-representation

Semi-discretized problem

$$\begin{bmatrix} M & & \\ & \ddots & \\ & & M \end{bmatrix} \begin{bmatrix} \dot{u}_1 \\ \vdots \\ \dot{u}_{d+2} \end{bmatrix} - \begin{bmatrix} \mathbf{C} & & \\ & \ddots & \\ & & \mathbf{C} \end{bmatrix} \begin{bmatrix} \mathbf{f}_1^\top \\ \vdots \\ \mathbf{f}_{d+2}^\top \end{bmatrix} + \begin{bmatrix} \mathbf{S} & & \\ & \ddots & \\ & & \mathbf{S} \end{bmatrix} \begin{bmatrix} \mathbf{f}_1^{b^\top} \\ \vdots \\ \mathbf{f}_{d+2}^{b^\top} \end{bmatrix} = 0$$

Constant coefficient matrices

$$M = \left[\int_{\Omega} B_i B_j \, d\Omega \right]_{i,j} \quad \mathbf{C} = \left[\int_{\Omega} \nabla B_i B_j \, d\Omega \right]_{i,j} \quad \mathbf{S} = \left[\int_{\Gamma} B_i B_j \mathbf{n} \, ds \right]_{i,j}$$

Stabilization of convective term by **Algebraic Flux Correction**⁴

⁴Kuzmin, MM, Gurrus, AFC II. In: Flux-Corrected Transport, Springer, 2012

Linearized FCT⁵

① Perform variational mass lumping $M \rightarrow M_l = \text{diag}\{m_i\}$

$$m_i := \int_{\Omega} \varphi_i(\mathbf{x}) \, d\Omega = \int_{\hat{\Omega}} \hat{B}_i(\boldsymbol{\xi}) |\det D\hat{G}| \, d\boldsymbol{\xi} > 0$$

Since

- B-spline basis functions satisfy PU property $\sum_j \hat{B}_j(\boldsymbol{\xi}) \equiv 1$
- $\det D\hat{G} > \text{tol} > 0$ by design of the grid generation algorithm
- B-spline basis functions $\hat{\varphi}_i(\boldsymbol{\xi}) > 0$ over their entire support

⁵Kuzmin, MM, Shadid, Shashkov, JCP 229 (2010) 8766-8779.

Linearized FCT⁵

- ① Perform variational mass lumping $M \rightarrow M_l = \text{diag}\{m_i\}$
- ② **Eliminate all negative eigenvalues from the flux-Jacobian**

$$R_i^{\text{high}} := \sum_j \mathbf{c}_{ij} \cdot \mathbf{F}_j = \sum_{j \neq i} \mathbf{e}_{ij} \cdot \mathbf{A}_{ij}^{\text{Roe}} (U_j - U_i), \quad \mathbf{e}_{ij} = 0.5(\mathbf{c}_{ij} - \mathbf{c}_{ji})$$

by adding artificial viscosities $D_{ij} := \|\mathbf{e}_{ij}\| R_{ij} |\Lambda_{ij}| R_{ij}^{-1}$

$$R_i^{\text{low}} := \sum_{j \neq i} [\mathbf{e}_{ij} \cdot \mathbf{A}_{ij}^{\text{Roe}} + D_{ij}] (U_j - U_i)$$

⁵Kuzmin, MM, Shadid, Shashkov, JCP 229 (2010) 8766-8779.

Linearized FCT⁵

- ① Perform variational mass lumping $M \rightarrow M_l = \text{diag}\{m_i\}$
- ② Eliminate all negative eigenvalues from the flux-Jacobian
- ③ **Solve** $M_l \dot{U}^{\text{low}} = R^{\text{low}} + S^{\text{low}}$ by an explicit SSP-RK method

$$M_l U^{(1)} = M_l U^n + \Delta t [R^n + S^n]$$

$$M_l U^{\text{low}} = \frac{1}{2} M_l U^n + \frac{1}{2} \left(M_l U^{(1)} + \Delta t [R^{(1)} + S^{(1)}] \right)$$

⁵Kuzmin, MM, Shadid, Shashkov, JCP 229 (2010) 8766-8779.

Linearized FCT⁵

- ① Perform variational mass lumping $M \rightarrow M_l = \text{diag}\{m_i\}$
- ② Eliminate all negative eigenvalues from the flux-Jacobian
- ③ Solve $M_l \dot{U}^{\text{low}} = R^{\text{low}} + S^{\text{low}}$ by an explicit SSP-RK method
- ④ **Linearize antidiffusive fluxes about the low-order predictor**

$$F_{ij} := m_{ij}(\dot{U}_i^{\text{low}} - \dot{U}_j^{\text{low}}) + D_{ij}^{\text{low}}(U_i^{\text{low}} - U_j^{\text{low}})$$

⁵Kuzmin, MM, Shadid, Shashkov, JCP 229 (2010) 8766-8779.

Linearized FCT⁵

- ① Perform variational mass lumping $M \rightarrow M_l = \text{diag}\{m_i\}$
- ② Eliminate all negative eigenvalues from the flux-Jacobian
- ③ Solve $M_l \dot{U}^{\text{low}} = R^{\text{low}} + S^{\text{low}}$ by an explicit SSP-RK method
- ④ Linearize antidiffusive fluxes about the low-order predictor
- ⑤ **Apply a generalized version of Zalesak's multidimensional 'nodal' flux limiter to scalar indicator variables ρ and p ($p > 0 \Rightarrow \rho E > 0$) and add a limited antidiffusive correction**

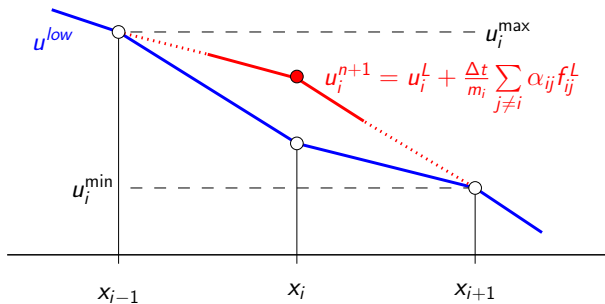
$$U_i^{n+1} = U_i^{\text{low}} + \frac{\Delta t}{m_i} \sum_{j \neq i} \min\{\alpha_{ij}^\rho, \alpha_{ij}^p\} F_{ij}$$

⁵Kuzmin, MM, Shadid, Shashkov, JCP 229 (2010) 8766-8779.

Zalesak's nodal FCT limiter⁶

'Nodal' flux limiter for $u \in \{\rho, p\}$ is designed to ensure that for all i

$$\min_{j:m_{ij} \neq 0} u_j^{\text{low}} =: u_i^{\text{min}} \leq u_i^{n+1} \leq u_i^{\text{max}} := \max_{j:m_{ij} \neq 0} u_j^{\text{low}}$$



⁶S. Zalesak, JCP 1979, 31(3), pp. 335–362

Positivity proof for B-spline based IgA

Theorem

When the same constraints are imposed on the *weights* of the B-spline function then the end-of-step solution stays within the upper and lower bounds set up by the low-order predictor.

Proof: Note that it is not the coefficients u_j^{\min} that are the local bounds (as in nodal FEM) but the functions $u^{\max}(\mathbf{x}) = \sum_j u_j^{\min} \varphi_j(\mathbf{x})$.

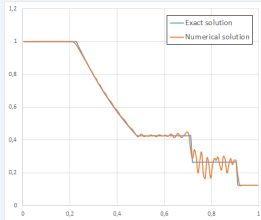
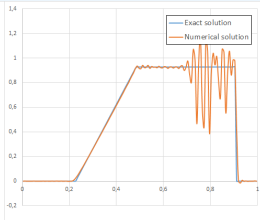
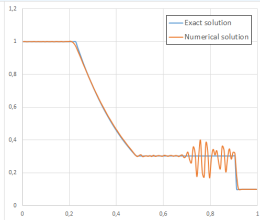
Assume that for some $\mathbf{x}^* \in \Omega$ we have $u^{n+1}(\mathbf{x}^*) > u^{\max}(\mathbf{x}^*)$:

$$0 > u^{\max}(\mathbf{x}^*) - u^{n+1}(\mathbf{x}^*) = \sum_j [\underbrace{u_j^{\max} - u_j^{n+1}}_{>0} \underbrace{\varphi_j(\mathbf{x}^*)}_{>0}] > 0$$

q.e.d.

Numerical examples

Sod's shock tube problem⁷

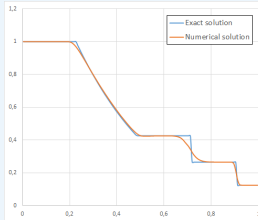
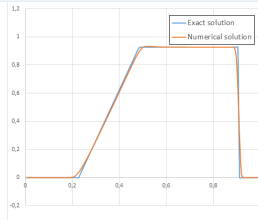
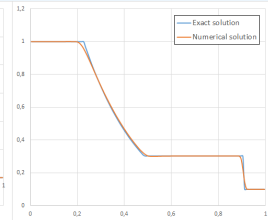
 ρ  v_x  p

Quadratic bi-variate B-spline basis functions with expl. SSP-RK(2).

⁷G.A. Sod, JCP 27 (1978) 1–31.

Numerical examples

Sod's shock tube problem⁷

 ρ  v_x  p

Quadratic bi-variate B-spline basis functions with expl. SSP-RK(2).

⁷G.A. Sod, JCP 27 (1978) 1–31.

Overview

1 Introduction

Scientific computing from a hardware perspective
Isogeometric design-simulation-optimization loop

2 Elliptic 'grid' generation

[J. Hinz]

Planar parameterizations
Volumetric parameterizations

3 Compressible flow solver

[A. Jaeschke]

Problem formulation
Linearized FCT limiter
Numerical examples

4 Implementation aspects

Meta-programming techniques for heterogeneous HPC

Meta-programming techniques for heterogeneous HPC

Strategy: Implement **one** device-independent single-patch compute kernel and just-in-time compile it into hardware-, formulation- and algorithm-optimized dynamically loadable libraries per patch

Computational building blocks

- Open-Source IGA library G+Smo⁸ (JKU, RICAM)
- 3rd party linear algebra libraries: ArrayFire, Blaze, Eigen, VexCL, ...
- Fluid Dynamics Building Blocks expression templates library⁹

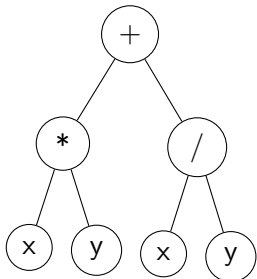
⁸<https://gs.jku.at/trac/gismo>

⁹<https://gitlab.com/mmoelle1/FDBB>

Expression templates

Code that you write

```
vex::vector<float> x,y,z;  
auto expr = x*y + x/y;  
  
z = expr;
```



All arithmetic operations are kept symbolically as [expression tree](#) whose evaluation is delayed until the assignment to the vector z. All arithmetic operation are then fused into a single evaluation (=loop).

Expression templates, cont'd

Compute kernel from VexCL

```
kernel void vexcl_vector_kernel (...)
{
    for (size_t idx = get_global_id(0);
          idx < n;
          idx += get_global_size(0))
    {
        prm_1[idx] = prm_2[idx] * prm_3[idx]
                    + prm_2[idx] / prm_3[idx];
    }
}
```

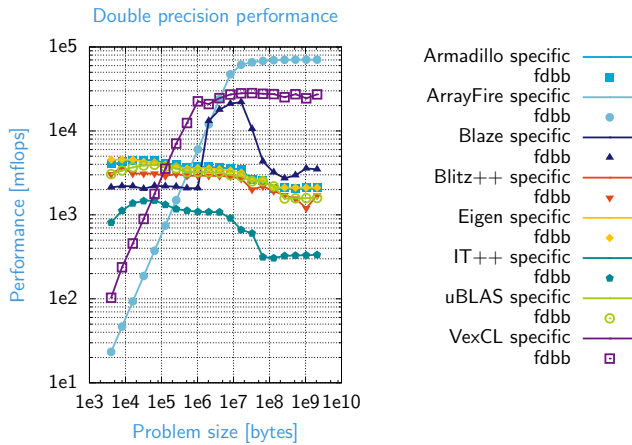
Fluid Dynamics Building Blocks

High-level	ET's for conservative/primitive variables, EOS, inviscid/ viscous fluxes, flux Jacobians, and Riemann invariants									
Low-level	Unified wrapper function API to core functionality of ETL's: make_temp, tag, tie, +, -, *, /, abs, sqrt, ...									
	Armadillo	ArrayFire	Blaze	Blitz++	Eigen	IT++	MTL4	uBLAS	VexCL	ViennaCL

FDBB μ -benchmark

$$y \leftarrow (m_x.*m_x + m_y.*m_y + m_z.*m_z)./(\rho.*\rho)$$

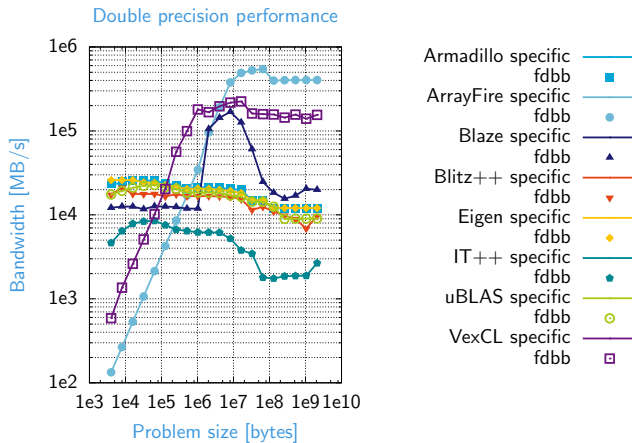
7 flop



FDBB μ -benchmark

$$y \leftarrow (m_x.*m_x + m_y.*m_y + m_z.*m_z)./(\rho.*\rho)$$

7 flop



Factory method design pattern

Code example: *single-patch inviscid fluxes*

```
1 using var = Variables<eos::idealGas<T>, dim,  
2                               EnumForm::conservative>;  
3 using fty = Factory<config, device>;  
4 auto    U = fty::stateVector<var>();  
5 auto    dF = fty::inviscidFluxes<var>();
```

- 1-2 The **Variable** typedef specifies all internals of the formulation like the equation of state, the spatial dimension, and the type of state vector variables (thereby defining fluxes and flux-Jacobians)

Factory method design pattern

Code example: *single-patch inviscid fluxes*

```
1  using var = Variables<eos::idealGas<T>, dim,  
2                                EnumForm::conservative>;  
3  using fty = Factory<config, device>;  
4  auto    U = fty::stateVector<var>();  
5  auto    dF = fty::inviscidFluxes<var>();
```

- 3 The **Factory** typedef selects optimal LA backend (Eigen, VexCL), data structures (SoA, AoS) and matrix formats (CSR, ELL, Band) for the particular **device** and problem **config**.

Factory method design pattern

Code example: *single-patch inviscid fluxes*

```
1 using var = Variables<eos::idealGas<T>, dim,  
2                                EnumForm::conservative>;  
3 using fty = Factory<config, device>;  
4 auto    U = fty::stateVector<var>();  
5 auto    dF = fty::inviscidFluxes<var>();
```

- 4-5 Vector and operator objects are created from the **Factory** typedef delegating memory allocation, etc. to the underlying LA backend

Factory method design pattern

Code example: *single-patch inviscid fluxes*

```
1 using var = Variables<eos::idealGas<T>, dim,  
2                               EnumForm::conservative>;  
3 using fty = Factory<config, device>;  
4 auto    U = fty::stateVector<var>();  
5 auto    dF = fty::inviscidFluxes<var>();
```

The `operator*` is overloaded such that `dF*U` unfolds to the SpMV representation of the discretized $\nabla \cdot \mathbf{F}(U)$ term, whereby fluxes, eos, etc. are implemented as lightweight expression templates in FDBB.

Factory method design pattern

Code example: *single-patch inviscid fluxes*

```
1  using var = Variables<eos::idealGas<T>, dim,
2                                EnumForm::conservative>;
3  using fty = Factory<config, device>;
4  auto    U = fty::stateVector<var>();
5  auto    dF = fty::inviscidFluxes<var>();
```

Is it worth the effort? Yes, because you can tune the implementation 'behind the scenes', e.g., by switching from AoS to SoA, i.e.

$\text{SpMatrix} < \text{T} \rangle \ C[\dim]; \rightarrow \text{SpMatrix} < \text{CST} < \text{T}, 1, \dim \rangle > \ C;$
 $\text{Vector} < \text{T} \rangle \ U[\dim + 2]; \rightarrow \text{Vector} < \text{CST} < \text{T}, \dim + 2, 1 \rangle > \ U;$

to save memory and computing time by factor $O(\dim)$.

Topics discussed:

- Parameterizations for screw machines with variable pitch
- Positivity-preserving IGA-solver for compressible flows
- Efficient implementation for heterogeneous HPC systems

Future work:

- THB-splines for solution-adapted parameterizations

Acknowledgements:

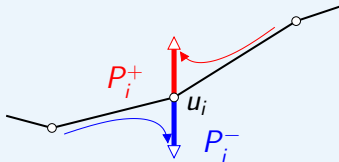
B. Jüttler, A. Mantzaflaris, D. Demidov, K. Igelberger

Financial support by EC under GA n° 678727 is acknowledged.



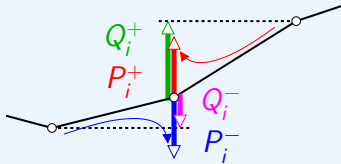
Zalesak's flux limiter¹⁰

- Consider sums of positive/negative antidiffusive fluxes into each node



¹⁰S. Zalesak, JCP 1979, 31(3), pp. 33 5–362

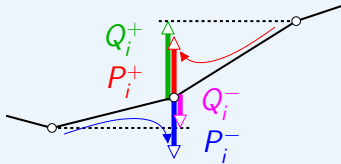
Zalesak's flux limiter¹⁰



- Consider sums of positive/negative antidiffusive fluxes into each node
- Limit antidiffusive flux if it exceeds the distance to upper/lower bounds

¹⁰S. Zalesak, JCP 1979, 31(3), pp. 33 5–362

Zalesak's flux limiter¹⁰



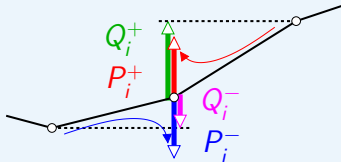
- Consider sums of positive/negative antidiffusive fluxes into each node
- Limit antidiffusive flux if it exceeds the distance to upper/lower bounds

- Compute nodal correction factors

$$R_i^+ = \min\{1, Q_i^+/P_i^+\} \quad \text{and} \quad R_i^- = \min\{1, Q_i^-/P_i^-\}$$

¹⁰S. Zalesak, JCP 1979, 31(3), pp. 33 5–362

Zalesak's flux limiter¹⁰



- Consider sums of **positive/negative** antidiffusive fluxes into each node
- Limit antidiffusive flux if it exceeds the distance to **upper/lower** bounds

- Compute nodal correction factors

$$R_i^+ = \min\{1, Q_i^+/P_i^+\} \quad \text{and} \quad R_i^- = \min\{1, Q_i^-/P_i^-\}$$

- Limit antidiffusive flux for edge ij by

$$\alpha_{ij} = \begin{cases} \min\{R_i^+, R_j^-\} & \text{for } \text{positive} \text{ fluxes} \\ \min\{R_i^-, R_j^+\} & \text{for } \text{negative} \text{ fluxes} \end{cases}$$

¹⁰S. Zalesak, JCP 1979, 31(3), pp. 33 5–362

Extended version of Zalesak's FCT limiter

Input: predictor u^L and antidiffusive fluxes f_{ij}^u , where $f_{ji}^u \neq f_{ij}^u$

- ① Sums of positive/negative antidiffusive fluxes into node i

$$P_i^+ = \sum_{j \neq i} \max\{0, f_{ij}^u\}, \quad P_i^- = \sum_{j \neq i} \min\{0, f_{ij}^u\}$$

- ② Upper/lower bounds based on the local extrema of u^L

$$Q_i^+ = m_i(u_i^{\max} - u_i^L), \quad Q_i^- = m_i(u_i^{\min} - u_i^L)$$

- ③ Correction factors $\alpha_{ij}^u = \alpha_{ji}^u$ to satisfy the FCT constraints

$$\alpha_{ij}^u = \min\{R_{ij}, R_{ji}\}, \quad R_{ij} = \begin{cases} \min\{1, Q_i^+ / P_i^+\} & \text{if } f_{ij}^u \geq 0 \\ \min\{1, Q_i^- / P_i^-\} & \text{if } f_{ij}^u < 0 \end{cases}$$

Node-based transformation of control variables¹¹

- **Conservative variables:** density, momentum, total energy

$$U_i = [\rho_i, (\rho \mathbf{v})_i, (\rho E)_i], \quad F_{ij} = [f_{ij}^\rho, \mathbf{f}_{ij}^{\rho v}, f_{ij}^{\rho E}], \quad F_{ji} = -F_{ij}$$

- **Primitive variables** $V = TU$: density, velocity, pressure

$$V_i = [\rho_i, \mathbf{v}_i, p_i], \quad \mathbf{v}_i = \frac{(\rho \mathbf{v})_i}{\rho_i}, \quad p_i = (\gamma - 1) \left[(\rho E)_i - \frac{|(\rho \mathbf{v})_i|^2}{2\rho_i} \right]$$

$$G_{ij} = [f_{ij}^\rho, \mathbf{f}_{ij}^v, f_{ij}^p] = T(U_i)F_{ij}, \quad T(U_j)F_{ji} = G_{ji} \neq -G_{ij}$$

- Raw antidiffusive fluxes for the velocity and pressure

$$\mathbf{f}_{ij}^v = \frac{\mathbf{f}_{ij}^{\rho v} - \mathbf{v}_i f_{ij}^\rho}{\rho_i}, \quad f_{ij}^p = (\gamma - 1) \left[\frac{|\mathbf{v}_i|^2}{2} f_{ij}^\rho - \mathbf{v}_i \cdot \mathbf{f}_{ij}^{\rho v} + f_{ij}^{\rho E} \right]$$

¹¹Kuzmin, MM, Shadid, Shashkov, JCP 229 (2010) 8766-8779.